Porous Coordination Polymers

DOI: 10.1002/ange.200904379

Oxidative Addition of Halogens on Open Metal Sites in a Microporous Spin-Crossover Coordination Polymer**

Gloria Agustí, Ryo Ohtani, Ko Yoneda, Ana B. Gaspar, Masaaki Ohba, Juan F. Sánchez-Royo, M. Carmen Muñoz, Susumu Kitagawa,* and José A. Real**

The last decade has witnessed a great activity in the realm of porous coordination polymers (PCPs). Their extreme chemical versatility and porosity has allowed chemists to consider PCPs as a new class of functional materials that are able to mimic, and even improve, the functions of zeolites, for example, storage, separation, and heterogeneous catalysis.[1] Furthermore, implementation of PCPs with solid-state properties (optical, magnetic, charge transport, etc.) would enable the expression of host–guest interactions in sorption and desorption processes in a sensory way as a response of the framework producing drastic physicochemical changes at ordinary temperatures. This almost unexplored strategy could provide a new generation of PCP-based sensors.[2]

The chemo-responsive behavior of the Hofmann clathrate PCPs $\{Fe(pz)[M^{II}(CN)_4]\}$ (**1**) (pz = pyrazine; M^{II} = Ni,[3a,b] Pd,[3a] Pt[3a]) based on the spin-crossover properties of the Fe^{II} joints was recently demonstrated. The cooperative response mediated by the components of the framework confers bistable behavior to the solid at room temperature. These PCPs form a 3D pillared-layer-type porous framework consisting of cyano-bridged $Fe^{II}M^{II}$ layers and pz pillar ligands, and adsorb various guest molecules. A bimodal reversible change of spin state at the Fe^{II} sites was observed concomitantly with the uptake of guest molecules switching between the high-spin state (HS, yellow), stabilized by hydroxylic solvents and five- and six-membered aromatic molecules, and the low-spin state (LS, red-brown), stabilized by CS_2 (for M = Pt)[3a] or CH_3CN (for M = Ni)[3b] at 298 K. In the framework, guest molecules can interact with the pyrazine pillar ligands (site A) and the M^{II} centers (site B).

One important feature not yet explored in these PCPs is the coordinative unsaturation of the M^{II} centers. Incorporation of coordinatively unsaturated metal centers, so-called "open metal sites", may enhance the adsorptive selectivity for particular guest substances.[4] Herein we report the chemisorptive uptake of dihalogen molecules involving associative oxidation of Pt^{II} to Pt^{IV} and reduction of the dihalogen to the corresponding halide to give $\{Fe(pz)[Pt(CN)_4(X)_p]\}$ [$X = Cl^-$ ($p = 1$), Br^- ($p = 1$), I^- ($0 \le p \le 1$)] (**2**). The consequences that these chemical changes have on the cooperative spin transition of the parent compound **1** are also presented and discussed.

Black-violet single crystals of $\{Fe(pz)[Pt(CN)_4(I)_p]\}$ (**2I**) with full occupation of I^- ($p = 1$)—the so-called α-phase—were obtained in a single-crystal-to-single-crystal transformation from orange-yellow single crystals of **1** in the HS state soaked in an aqueous solution of I_3^- at 293 K (see the Supporting Information).[5] The structure of **2I** (α-phase) is closely related to that of **1** and **1**·2H_2O; it remains in the tetragonal *P*4/*mmm* space group, but with the typical crystal parameters of the LS state at 293 K. However, the crystal recovers the HS state, and the yellow color, at temperatures higher than 395 K (see below and Table S1 in the Supporting Information) and consists of planar $\{Fe[Pt(CN)_4]\}_\infty$ layers defined by axially distorted octahedra of Fe^{II} ions interconnected through the equatorial positions by $[Pt(CN)_4]^{n-}$ moieties (Figure 1). The axial positions of the Fe sites, which are collinear with the C_4 axis, are occupied by the bridging pyrazine ligands, which connect consecutive layers. The equatorial and axial Fe–N bond lengths are consistent with the LS and the HS states, respectively [$Fe–N_{eq}$ 1.940(6) and $Fe–N_{ax}$ 2.001(12) Å at 293 K, and $Fe–N_{eq}$ 2.127(8) and $Fe–N_{ax}$ 2.275(14) Å at 413 K]. The axial positions of the Pt centers, which are available in the so-called site B, are coordinated by two iodide anions with half occupancy. The

[*] Dr. G. Agustí, Dr. A. B. Gaspar, Prof. Dr. J. A. Real
Instituto de Ciencia Molecular (ICMol)/
Departamento de Química Inorgánica, Universidad de Valencia
Edificio de Institutos de Paterna
Apartado de correos 22085, 46071 Valencia (Spain)
E-mail: jose.a.real@uv.es
Prof. Dr. M. C. Muñoz
Departamento de Física Aplicada, Universitad Politécnica de Valencia, Camino de Vera s/n, 46022 Valencia (Spain)
Dr. J. F. Sánchez-Royo
Instituto de Ciencia de los Materiales de la Universidad de Valencia
Universidad de Valencia, Doctor Moliner 50
46100 Burjassot Valencia (Spain)
R. Ohtani, K. Yoneda, Dr. M. Ohba, Prof. Dr. S. Kitagawa
Department of Synthetic Chemistry and Biological Chemistry
Graduate School of Engineering, Kyoto University Katsura
Nishikyo-ku, Kyoto 615-8510 (Japan)
E-mail: ohba@sbchem.kyoto-u.ac.jp
kitagawa@sbchem.kyoto-u.ac.jp
Dr. M. Ohba, Prof. Dr. S. Kitagawa
RIKEN Spring-8 Center, Kouto, Sayo-cho, Sayo-gun
Hyogo 679-5198 (Japan)
Prof. Dr. S. Kitagawa
Institute for Integrated Cell-Material Sciences (iCeMS), Yoshida
Sakyo-ku, Kyoto 606-8501 (Japan)

[**] This work was supported by a ERATO JST Project "Kitagawa Integrated Pore Project", CREST JST, the Spanish Ministerio de Ciencia e Innovación (MICINN) and FEDER funds, (CTQ2007-64727) and the Generalitat Valenciana funds (ACOMP/2009/326). A.B.G. thanks the MICINN for a Ramon y Cajal research contract. G.A. thanks the network MAGMANet, a network of excellence of the European Union (Contract: NMP3-CT-2005-515767-2) for a predoctoral grant.

Supporting information for this article is available on the WWW under http://dx.doi.org/10.1002/anie.200904379.

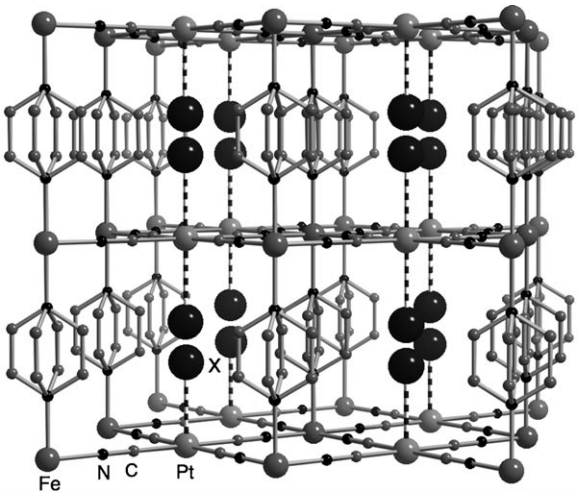

Figure 1. Representative fragment of the **2X** structure (X = Cl, Br, I; the occupancy of the X atoms is 0.5, and the Pt atoms are in a Pt^{II}/Pt^{IV} mixed-valence state). The pyrazine ligands are disordered about the C_4 axis.

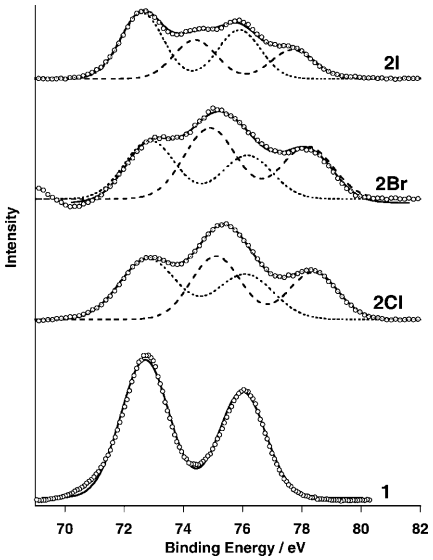

Figure 2. Platinum 4f region of the X-ray photoelectron spectrum for **1** and **2X** [X = Cl, Br, I (α-phase)]. The solid lines correspond to the best deconvolution of the experimental data. Dotted and broken lines represent the Pt^{II} and Pt^{IV} components, respectively.

Pt–I bond lengths [2.714(3) Å at 293 K and 2.702(3) Å at 413 K] are within the limits usually found for Pt–I complexes.[6] On the basis of the I/Pt ratio, the Pt–I distance, the occupancy of the I atoms, and the XPS data (see below), a reasonable "static" picture is represented by an alternate arrangement of square-planar $[Pt^{II}(CN)_4]^{2-}$ and axially elongated octahedral $[Pt^{IV}(CN)_4(I)_2]^{2-}$ units in the framework (Figure S1 in the Supporting Information). However, no extra X-ray diffraction peaks attributed to the super lattice based on ordered arrangement of the Pt^{II} and Pt^{IV} units were observed. In this respect, it is important to note that the $[Pt^{II}(CN)_4]^{2-}$ and $[Pt^{IV}(CN)_4(X)_2]^{2-}$ units would be uniformly and randomly arrayed in the lattice, and the structure of the $[Pt(CN)_4]$ moiety is determined as a mixture of the Pt^{II} and Pt^{IV} species. Upon spin transition, the unit cell volume of **2I** (α-phase) changes by 56.5(2) $Å^3$ per Fe atom, a value consistent with complete transformation of the LS state to the HS state in **1**.

Isomorphous single crystals **2Br** and **2Cl** were synthesized by exposing single crystals of **1** to Br_2 and Cl_2 vapors, respectively (see the Supporting Information). At 293 K, the color of **2Br** is dark brown, whereas **2Cl** remains yellow, denoting the stabilization of the LS and HS states, respectively. The structures were solved as the LS form at 150 K to minimize positional disorder, which is particularly important for Cl atoms in **2Cl**. The $Fe–N_{eq}$ and $Fe–N_{ax}$ bond lengths are 1.92(2) (**2Br**) and 1.9084(6) Å (**2Cl**), and 1.97(2) (**2Br**) and 1.97(2) Å (**2Cl**), respectively, and the Pt–X bond lengths are 2.595(10) (**2Br**) and 2.600(11) Å (**2Cl**). Full structure determination of the HS forms of **2Br** and **2Cl** was unsuccessful most likely because of the poor quality of the crystals.

To examine the valence state of the Pt centers, XPS measurements in the region for 4f orbitals were made on samples of single crystals of **1** (as reference compound) and **2X** (X = Cl, Br, I) at 293 K (Figure 2). Compound **1** displays a $4f_{7/2}$, $4f_{5/2}$ doublet with binding energies (BE) of approximately 72.8 and 76.0 eV. The $4f_{7/2}$ BE is markedly smaller than that found for the parent $K_2[Pt^{II}(CN)_4]$ complex (BE-$(4f_{7/2}) = 74.2$ eV).[7] In general, a decrease of the BE energy can be associated with Pt metal sites coordinating electron donor ligands.[8] For **1**, the only possible electron donor source is the $Fe^{II}–N{\equiv}C–Pt^{II}$ interaction, more precisely the π back-bonding donation from the Fe^{II} ion to the $[Pt^{II}(CN)_4]^{2-}$ group. Experimental evidence of such covalent coupling was obtained from the strong dependence of some fundamental vibrational modes of $[Pt^{II}(CN)_4]^{2-}$ on the spin state of Fe^{II}.[9] Pt 4f spectra measured in the compounds **2X** show broadening and the appearance of a shoulder at higher energies, which is evidence of two Pt 4f doublets in these compounds. Deconvolution of these spectra was performed by assuming that each doublet is defined by two peaks of the same width with an intensity ratio given by the relative $(2J+1)$ degeneracy of the electronic states and with the same spin–orbit splitting as that measured for compound **1**. The binding energies associated to both components BE_1 and BE_2 are shown in Table 1.

The BE energies of the first doublet are close to those of the reference compound **1**, so this doublet is attributed to a Pt^{II} site. The second doublet, which is shifted to higher energies by around 2 eV, indicates the presence of Pt^{IV} sites. However, the BE_2 doublet appears at energies remarkably smaller than the corresponding ones observed for the related complexes $K_2[Pt^{IV}(CN)_4(Cl)_2]\cdot 3H_2O$ $(BE(4f_{7/2}) = 76.3$ eV)[7]

Table 1: Binding energies (BE) [eV] for the 4f region of Pt.

Compound	BE_1		BE_2	
	$4f_{7/2}$	$4f_{5/2}$	$4f_{7/2}$	$4f_{5/2}$
1	72.8	76.0	–	–
2Cl	72.8	76.1	75.1	78.4
2Br	72.9	76.2	74.9	78.2
2I	72.6	75.9	74.4	77.7

and $K_2[Pt^{IV}(CN)_6]$ ($BE_2(4f_{7/2}) = 76.8$ eV),[10] and it shifts by around 0.7 eV to smaller energies when moving from **2Cl** to **2I** (α-phase), a fact that can be related to the electronegativity of X.[8,11]

The Pt^{II}:Pt^{IV} ratio, estimated from the relative intensity of the doublets, indicates that during the first minute of irradiation the measured amount of Pt^{IV} was found to be around 50% for the three derivatives. However, the amount of the Pt^{IV} decreases as irradiation time increases. Thus, after one hour the relative amount of Pt^{IV} is 10–20% smaller. This imbalance of the Pt^{II}:Pt^{IV} ratio is related to the capacity of soft X-ray photons to reduce Pt^{IV} to Pt^{II}.[12] Therefore, what we observe is a reductive elimination of the halide provoked by the X-ray photons (Figure S2 in the Supporting Information). The halide nature of the X atom was confirmed by XPS experiments [I^-: $BE(4d_{3/2}) = 618.6$ eV, $BE(4d_{1/2}) = 630.0$ eV; Br^-: $BE(3d_{3/2}) = 67.8$ eV; Cl^-: $BE(2p) = 197.8$ eV; Figure S3 in the Supporting Information). In summary, these results are consistent with a "static" picture in which the structure of **2X** would correspond to an alternating distribution of $[Pt^{II}(CN)_4]^{2-}$ and $[Pt^{IV}(CN)_4(X)_2]^{2-}$ units (Figure S1).

Furthermore, our XPS results are sensitive to changes of Fe^{II} spin state. At 298 K, the maxima of the Fe^{II} $2p_{3/2}$ XPS signal for **1**, **2Cl**, **2Br**, and **2I** appear at 709.8, 709.6, 708.5, and 708.3 eV, respectively (Figure S4 in the Supporting Information). There is a difference of around 1.3 eV between the HS state represented by **1** and **2Cl** and the LS state represented by **2Br** and **2I** (α-phase).

The thermal dependence of $\chi_M T$ (χ_M is the molar magnetic susceptibility and T the temperature) of samples of single crystals of **2X** is displayed in Figure 3. Below 240 K, $\chi_M T$ adopts values for the three derivatives in the range 0.3–0.5 $cm^3 K mol^{-1}$, which is consistent with the Fe^{II} ion in the LS state and with the presence of a residual amount (8–14%) of Fe^{II} ions in the HS state. On heating of the sample, $\chi_M T$ increases sharply to reach values around 3.6 $cm^3 K mol^{-1}$, which is typical for the Fe^{II} ion in the HS state. The critical temperatures are $T_c^{(up)} = 270$ K (**2Cl**), 324 K (**2Br**), and 392 K (**2I** α-phase). In the cooling mode, the critical temperatures, $T_c^{(down)} = 258$ K (**2Cl**), 293 K (**2Br**), and 372 K (**2I** α-phase), show hysteresis loops with widths of 12–31 K. The spin transition is accompanied by a drastic change of color from dark violet (**2I**), dark brown (**2Br**), deep red (**2Cl**) in the LS state to yellow-orange in the HS state.

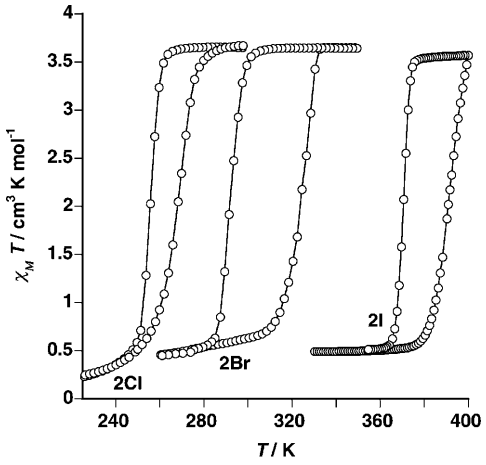

Figure 3. $\chi_M T$ versus T plots for **2Cl**, **2Br**, and **2I** (α-phase).

The trend shown by the T_c values reveals the sensitivity of the Fe^{II} coordination core to the "availability" of the lone electron pair cloud of the nitrogen atom in the Fe–NC–Pt–X moiety. The σ-donor capability of the nitrogen atom decreases as the electronegativity of X^- increases, inducing a decrease of the ligand field and the value of T_c. This conjecture is supported by the downward shift of the Pt^{IV} 4f BE_2 doublet when moving from **2Cl** to **2I**.

When microcrystalline samples of **1** were exposed to vapor of I_2, a new phase of **2I**, the so-called β-phase, was obtained. This phase, characterized by $p \approx 0.6$, has practically the same powder X-ray pattern as **1** and **2I** (α-phase) in the LS state (Figure S5 in the Supporting Information). Also, **2I** (β-phase) shows essentially same XPS pattern of **2I** (α-phase) with lower I/Pt and Pt^{IV}/Pt^{II} ratios. The representative magnetic behavior of the **2I** (β-phase) is shown in Figure 4

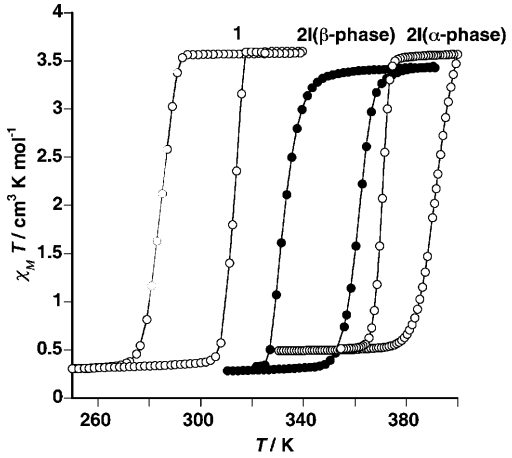

Figure 4. $\chi_M T$ versus T plots of **1**, **2I** (β-phase, $p \approx 0.6$), and **2I** (α-phase, $p = 1$).

together with that of **1** and **2I** (α-phase). The β-phase undergoes a cooperative spin transition with critical temperatures $T_c^{(down)} = 331$ K and $T_c^{(up)} = 360$ K for the cooling and warming modes, respectively. The critical temperatures $T_c^{(down)}$ and $T_c^{(up)}$ are higher by 46 and 51 K, respectively, than the corresponding values for the free guest network **1**, and 41 and 32 K lower than those of **2I** (α-phase), which suggests that I atoms distribute homogeneously in the β-phase framework and the critical temperatures of **2I** depend on the I content (Figure 4). Compound **2I** (β-phase) was consistently obtained with $p \approx 0.6$, whereas similar β-phases for **2Br** and **2Cl** have not yet been clearly identified. The most important difficulty is the reliability of the samples because of the higher reactivity of the microcrystalline powders **1** with Br_2 and Cl_2 gases.

We have demonstrated that the PCP $\{Fe(pz)[Pt^{II}(CN)_4]\}$ (**1**) efficiently adsorbs halogen molecules X_2 (X = Cl, Br, I) thanks to the presence in the pores providing $[Pt(CN)_4]^{2-}$ units as "open metal sites" that are able to undergo oxidative addition of X atoms. In the particular case of iodine,

chemisorption takes place from aqueous solution or vapor with strong stabilization of the LS state and accompanied by a remarkable change of color from yellow to black-violet, which could be useful for sequestering and sensing iodine. Understanding how the PCPs sequester iodine may be helpful for evaluating and developing methods for minimizing environmental effects.

Experimental Section

X-ray diffraction data for **2I** (HS) and **2I** (LS) were collected on a Rigaku Varimax CCD system, and data for **2Cl**, **2Br**, and **2I**·2 H_2O were collected with a Nonius Kappa-CCD single-crystal diffractometer. CCDC 742860 (LS **2I**), 742861 (LS **2I**), 742863 (**2Cl**), 742864 (**2Br**), and 742865 (**2I**·2 H_2O) contain the supplementary crystallographic data for this paper. These data can be obtained free of charge from The Cambridge Crystallographic Data Centre via www.ccdc.cam.ac.uk/data_request/cif.

XPS measurements were carried out in an XPS Escalab 210 spectrometer from Thermo VG Scientific. The base pressure in the analysis chamber was 1.0×10^{-10} mbar. Photoelectrons were extracted by using the $Mg_{K\alpha}$ excitation line ($h\nu = 1253.6$ eV). Variable-temperature magnetic susceptibility measurements of all samples (20–30 mg) were recorded on a Quantum Design MPMS2 SQUID susceptometer equipped with a 5.5 T magnet operating at 1 T and in the 1.8–400 K temperature interval. The susceptometer was calibrated with $(NH_4)_2Mn(SO_4)_2 \cdot 12H_2O$. Experimental susceptibilities were corrected for diamagnetism of the constituent atoms by using Pascal's constants.

Received: August 5, 2009
Published online: October 23, 2009

Keywords: chemisorption · coordination polymers · oxidative addition · porous compounds · spin crossover

[1] a) C. Janiak, *Dalton Trans.* **2003**, 2781; b) S. Kitagawa, R. Kitaura, S-i Noro, *Angew. Chem.* **2004**, *116*, 2388; *Angew. Chem. Int. Ed.* **2004**, *43*, 2334; c) G. Férey, *Chem. Soc. Rev.* **2008**, *37*, 191.

[2] See, for example: a) J. A. Real, E. Andrés, M. C. Muñoz, M. Julve, T. Granier, A. Bousseksou, F. Varret, *Science* **1995**, *268*, 265; b) G. J. Halder, C. J. Kepert, B. Moubaraki, K. S. Murray, J. D. Cashion, *Science* **2002**, *298*, 1762; c) C. Serre, F. Pelle, N. Gardant, G. Ferey, *Chem. Mater.* **2004**, *16*, 1177; d) K. L. Wong, G. L. Law, Y. Y. Yang, W. T. Wong, *Adv. Mater.* **2006**, *18*, 1051; e) D. Tanaka, S. Horike, S. Kitagawa, M. Ohba, M. Hasegawa, Y. Ozawa, K. Toriumi, *Chem. Commun.* **2007**, 3142; f) B. Chen, Y. Yang, F. Zapata, G. Lin, G. Qian, E. B. Lobkovsky, *Adv. Mater.* **2007**, *19*, 1693; g) S. M. Neville, G. J. Halder, K. W. Chapman, M. B. Duriska, P. D. Southon, J. D. Cashion, J. F. Létard, B. Moubaraki, K. S. Murray, C. J. Kepert, *J. Am. Chem. Soc.* **2008**, *130*, 2869; h) A. Lan, K. Li, H. Wu, D. H. Olson, T. J. Emge, W. Ki, M. Hong, J. Li, *Angew. Chem.* **2009**, *121*, 2370; *Angew. Chem. Int. Ed.* **2009**, *48*, 2334.

[3] a) M. Ohba, K. Yoneda, G. Agustí, M. C. Muñoz, A. B. Gaspar, J. A. Real, M. Yamasaki, H. Ando, Y. Nakao, S. Sakaki, S. Kitagawa, *Angew. Chem.* **2009**, *121*, 4861; *Angew. Chem. Int. Ed.* **2009**, *48*, 4767; b) P. D. Southon, L. Liu, E. A. Fellows, D. J. Price, G. J. Halder, K. W. Chapman, B. Moubaraki, K. S. Murray, J. F. Létard, C. J. Kepert, *J. Am. Chem. Soc.* **2009**, *131*, 10998.

[4] a) B. Chen, N. Ockwig, A. R. Millward, D. S. Contreras, O. M. Yaghi, *Angew. Chem.* **2005**, *117*, 4823; *Angew. Chem. Int. Ed.* **2005**, *44*, 4745; b) S. Ma, H.-C. Zhou, *J. Am. Chem. Soc.* **2006**, *128*, 11734; P. M. Forster, J. Eckert, B. D. Heiken, J. B. Parise, J. W. Yoon, S. H. Jhung, J.-S. Chang, A. K. Cheetham, *J. Am. Chem. Soc.* **2006**, *128*, 16850; c) M. Dinca, A. Dailly, Y. Liu, C. M. Brown, D. A. Newmann, J. R. Long, *J. Am. Chem. Soc.* **2006**, *128*, 16876.

[5] Crystals of the dihydrate **2I**·2 H_2O were also formed by slow diffusion of the components in presence of I_3^- in water. The structure was solved at 180 K to avoid positional disorder. This dihydrate form is isostructural with **2I**; the two molecules of water interpose between the pz rings (site A). The Fe–N_{eq}, Fe–N_{ax}, and Pt–I bond lengths were found to be 1.9735(9), 2.02(4), and 2.738(8) Å, respectively (Table S1 and Figure S6 in the Supporting Information). At temperatures above 360 K, the dihydrate loses the two molecules of water to give **2I** (α-phase) (Figure S7). The magnetic behavior of this compound is shown in Figure S8.

[6] See, for example: C. Bellitto, A. Flamini, L. Gastaldi, L. Scaramuzza, *Inorg. Chem.* **1983**, *22*, 444; H. Iguchi, S. Takaishi, T. Kajiwara, H. Miyasaka, M. Yamashita, H. Matsuzaki, H. Okamoto, *J. Am. Chem. Soc.* **2008**, *130*, 17668; A. N. Westra, S. A. Bourne, C. Esterhuysen, K. R. Koch, *Dalton Trans.* **2005**, 2162.

[7] D. Cohen, J. E. Lester, *Chem. Phys. Lett.* **1973**, *18*, 109.

[8] C. Battocchio, I. Fratoddi, V. Russo, G. Polzonetti, *J. Phys. Chem. A* **2008**, *112*, 7365.

[9] G. Molnár, V. Niel, A. B. Gaspar, J. A. Real, A. Zwick, A. Bousseksou, J. J. McGarvey, *J. Phys. Chem. B* **2002**, *106*, 9701.

[10] J. Pei, L. Weng, X-y Li, *J. Electroanal. Chem.* **2000**, *480*, 74.

[11] S. Hüfner, *Photoelectron Spectroscopy*, *Vol. 82*, Springer, Berlin, **1995** (Springer Series in Solid-State Sciences).

[12] P. Burroughs, A. Hammett, J. F. McGilp, A. F. Orchard, *J. Chem. Soc. Faraday Trans.* **1975**, *71*, 177.

